

**Supplementary Information:****Phase transitions in confined water nanofilms**

Sungho Han,<sup>1</sup> M. Y. Choi,<sup>2,1</sup> Pradeep Kumar,<sup>3</sup> and H. Eugene Stanley<sup>1</sup>

*<sup>1</sup>Center for Polymer Studies and Department of Physics,  
Boston University, Boston, Massachusetts 02215, USA*

*<sup>2</sup>Department of Physics and Astronomy,  
Seoul National University, Seoul 151-747, Republic of Korea*

*<sup>3</sup>Center for Studies in Physics and Biology,  
The Rockefeller University, New York, New York 10021, USA*

## I. INVESTIGATION OF A HYSTERESIS LOOP IN POTENTIAL ENERGY UPON SLOW COOLING AND HEATING

To support that the nature of phase transitions for densities  $\rho < \rho_c$  and  $\rho > \rho_c$  is different, we investigate the existence of a hysteresis loop in the potential energy  $U$  during slow cooling and heating processes. In general, a continuous phase transition does not display a hysteresis loop in cooling and heating processes; accordingly, the existence of the hysteresis loop provides strong support for a first-order phase transition line.

Figure 1 in supplementary information shows a hysteresis loop in  $U$  for  $\rho < \rho_c$  upon cooling and heating. While at  $\rho = 1.16 \text{ g/cm}^3$  ( $< \rho_c$ ) we find a large hysteresis loop, the hysteresis loop tends to shrink as  $\rho$  approaches  $\rho_c$ . On the other hand, as presented in Fig. 2, we find that there is no hysteresis loop in  $U$  for  $\rho > \rho_c$ , during slow cooling and heating processes. Upon slow cooling or heating,  $U$  gradually decreases or increases without a hysteresis loop. Thus non-existence of a hysteresis loop in  $U$  upon cooling and heating processes for  $\rho > \rho_c$  strongly supports that the nature of the phase transition for  $\rho > \rho_c$  is different from the one for  $\rho < \rho_c$  which is a first-order transition showing a hysteresis loop in  $U$ .

## II. AVERAGE LATERAL PRESSURE VERSUS TEMPERATURE

Next, we calculate the average lateral pressure  $\langle P_{xy} \rangle$  in the  $NVT$  ensemble, which is the pressure in the parallel direction to the plates, as a function of temperature  $T$ . In Fig. 3, we show  $\langle P_{xy} \rangle$  versus  $T$  for  $\rho < \rho_c$ . When the system undergoes a phase transition to ice,  $\langle P_{xy} \rangle$  increases abruptly and also exhibits a hysteresis loop upon slow cooling and heating, showing the first-order character of the transition. Since the volume  $V$  of the system is kept fixed during simulations, it is reasonable that  $\langle P_{xy} \rangle$  abruptly increases during freezing. Namely, the abrupt change of  $\langle P_{xy} \rangle$  in the  $NVT$  ensemble corresponds to the discontinuity of  $\rho$  in the  $NP_{xy}T$  ensemble. For  $\rho > \rho_c$ , in contrast,  $\langle P_{xy} \rangle$  does not change abruptly in the cooling or heating process. Instead, as  $T$  is varied, it keeps changing continuously without a hysteresis loop in  $\langle P_{xy} \rangle$ , again demonstrating the difference in the nature of the phase transition for  $\rho > \rho_c$  and for  $\rho < \rho_c$ . This is fully consistent with the results in the main text, convincing us that the nature of phase transitions for  $\rho < \rho_c$  and  $\rho > \rho_c$  is different.

### III. $NP_{xy}T$ ENSEMBLE SIMULATIONS

From the calculation of the average lateral pressure  $\langle P_{xy} \rangle$  in the  $NVT$  ensemble, we estimate the critical lateral pressure  $P_c$  in the range  $1.0 \text{ GPa} < P_c < 1.2 \text{ GPa}$ , and perform molecular dynamics simulations in the  $NP_{xy}T$  ensemble for two different pressures  $P_{xy} < P_c$  and  $P_{xy} > P_c$ . Specifically, we choose  $P_{xy} = 540 \text{ MPa} (< P_c)$  and  $P_{xy} = 1.5 \text{ GPa} (> P_c)$ .

Figure 5 displays  $U$  versus  $T$ . Here we also observe that upon cooling there is an abrupt decrease in  $U$  for  $P_{xy} < P_c$  but rather a gradual decrease for  $P_{xy} > P_c$ . Similarly, in Fig. 6, there is a discontinuous change in  $\rho$  when water freezes for  $P_{xy} < P_c$ , but  $\rho$  changes continuously upon freezing for  $P_{xy} > P_c$ . Further, we find that the lateral oxygen–oxygen radial distribution function changes discontinuously and continuously when a phase transition occurs for  $P_{xy} < P_c$  and for  $P_{xy} > P_c$ , respectively (see Fig. 7).

Finally, we remark that all simulation results presented here are consistent with the results in the main text and they provide convincing evidences for the presence of two different phase transitions, first-order and continuous, between solid and liquid. The corresponding two phase boundaries meet at a point.

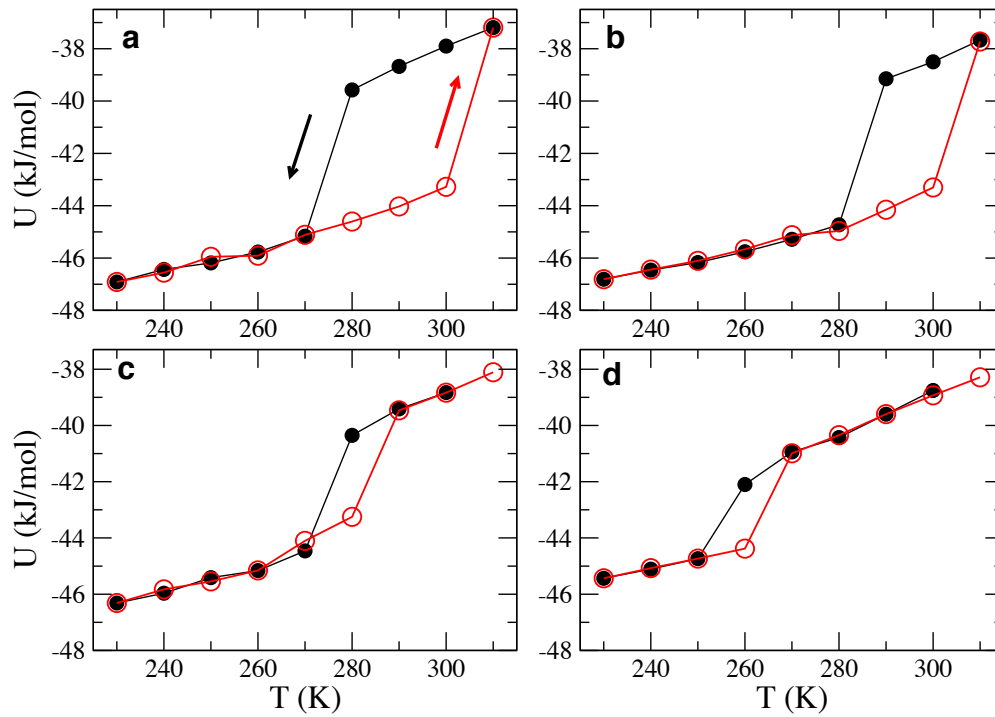


FIG. 1: Hysteresis loops in potential energy  $U$  during slow cooling (black filled circles) and heating (red unfilled circles) processes for  $\rho < \rho_c$ . The density for each panel is  $\rho =$  **a.**  $1.16 \text{ g/cm}^3$ , **b.**  $1.21 \text{ g/cm}^3$ , **c.**  $1.28 \text{ g/cm}^3$ , and **d.**  $1.30 \text{ g/cm}^3$ .

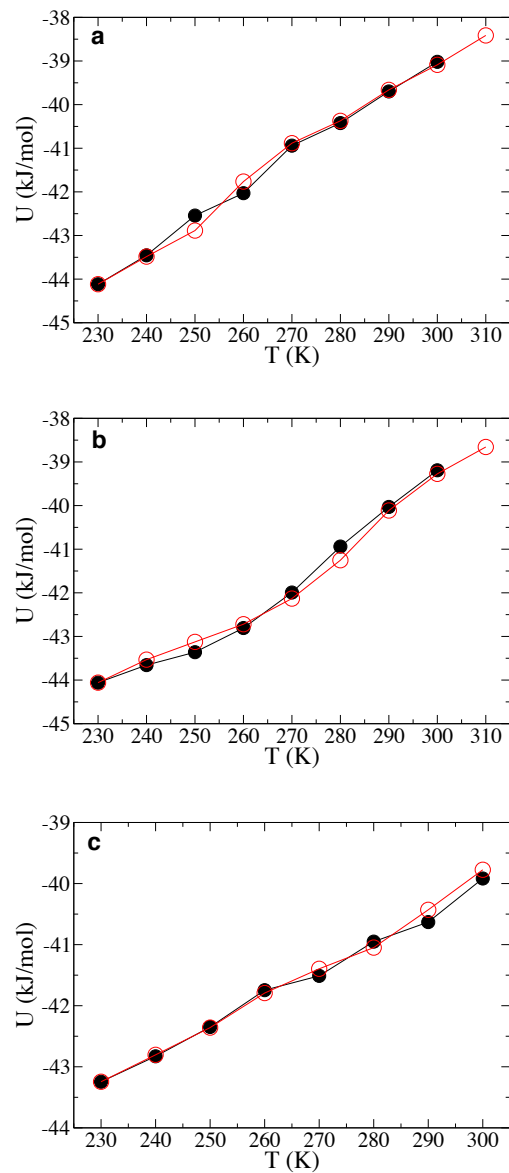


FIG. 2: Absence of a hysteresis loop in potential energy  $U$  during slow cooling and heating processes for  $\rho > \rho_c$ . The density for each panel is  $\rho =$  **a.** 1.33 g/cm<sup>3</sup>, **b.** 1.39 g/cm<sup>3</sup>, and **c.** 1.45 g/cm<sup>3</sup>. Symbols are the same as those in Fig. 1.

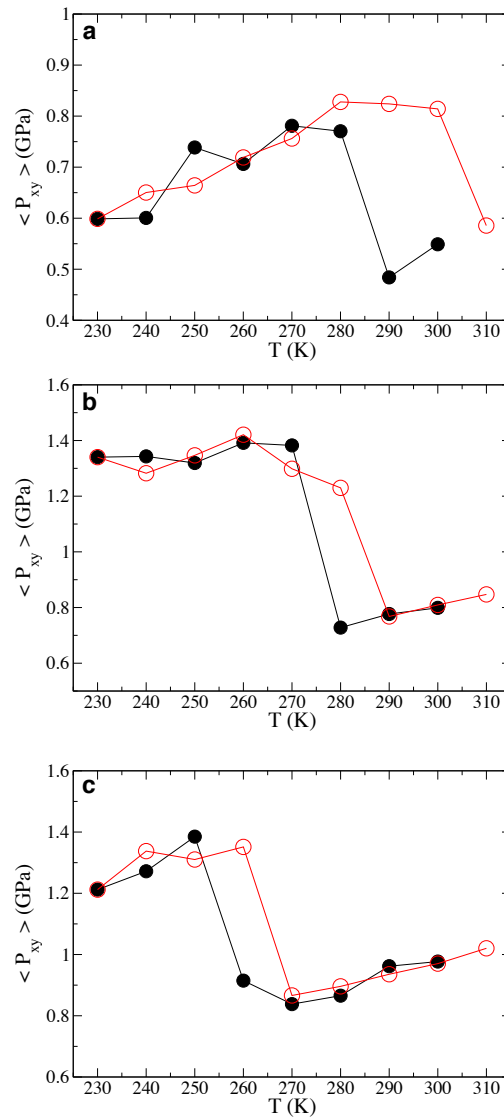


FIG. 3: Average lateral pressure  $\langle P_{xy} \rangle$  computed in the  $NVT$  ensemble as a function of temperature  $T$  for  $\rho < \rho_c$ . The density for each panel is  $\rho =$  **a.**  $1.21 \text{ g/cm}^3$ , **b.**  $1.28 \text{ g/cm}^3$ , and **c.**  $1.30 \text{ g/cm}^3$ . Symbols are the same as those in Fig. 1.

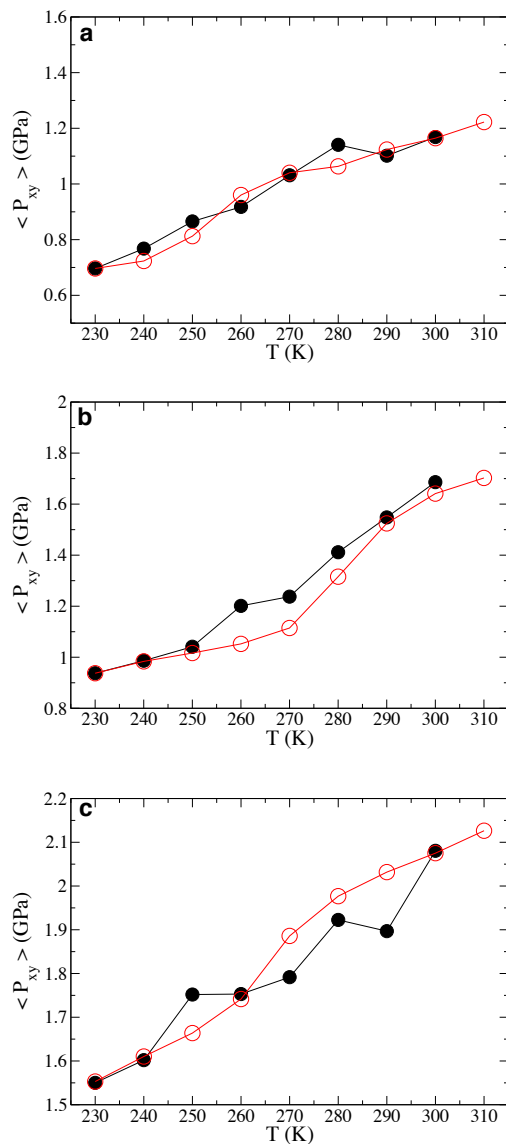


FIG. 4: Average lateral pressure  $\langle P_{xy} \rangle$  computed in the  $NVT$  ensembles as a function of temperature  $T$  for  $\rho > \rho_c$ . The density for each panel is  $\rho =$  **a.** 1.33 g/cm<sup>3</sup>, **b.** 1.39 g/cm<sup>3</sup>, and **c.** 1.45 g/cm<sup>3</sup>. Symbols are again the same as those in Fig. 1.

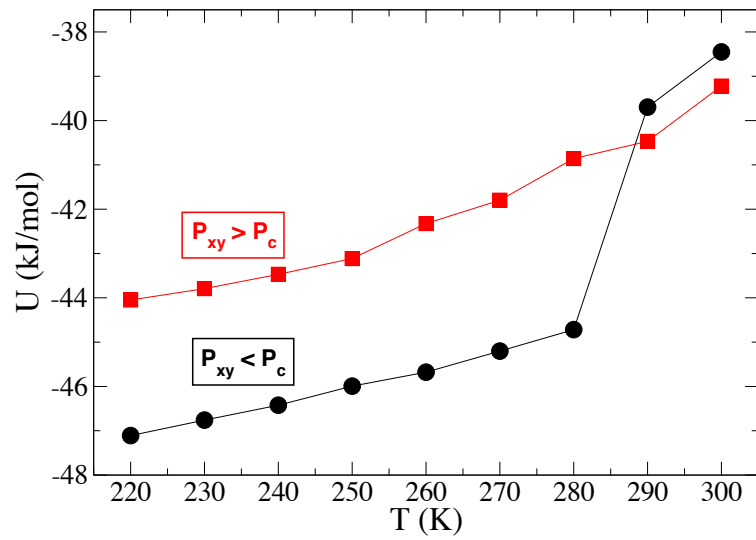


FIG. 5: Potential energy  $U$  versus temperature  $T$  upon cooling, for lateral pressure  $P_{xy} = 540 \text{ MPa} (< P_c)$  and  $1.5 \text{ GPa} (> P_c)$  in the  $NP_{xy}T$  ensemble. An abrupt drop in  $U$  is observed for  $P_{xy} < P_c$  as  $T$  is lowered. For  $P_{xy} > P_c$ , in contrast,  $U$  gradually decreases without an abrupt drop. This result is consistent with that in the  $NVT$  ensemble.



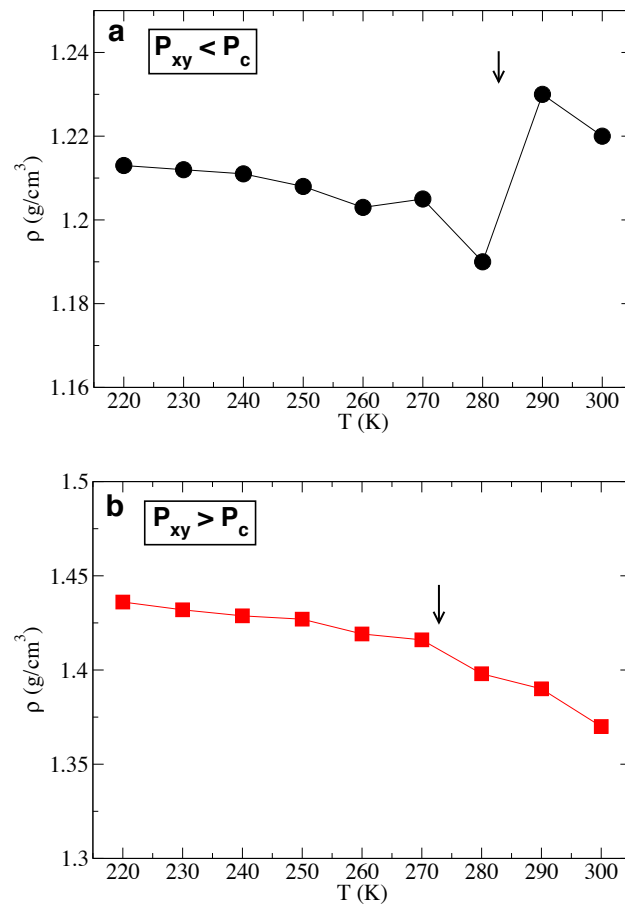


FIG. 6: Density  $\rho$  versus temperature  $T$  for **a.**  $P_{xy} < P_c$  and **b.**  $P_{xy} > P_c$ . When water freezes (designated by an arrow),  $\rho$  changes discontinuously for  $P_{xy} < P_c$  but continuously for  $P_{xy} > P_c$ .

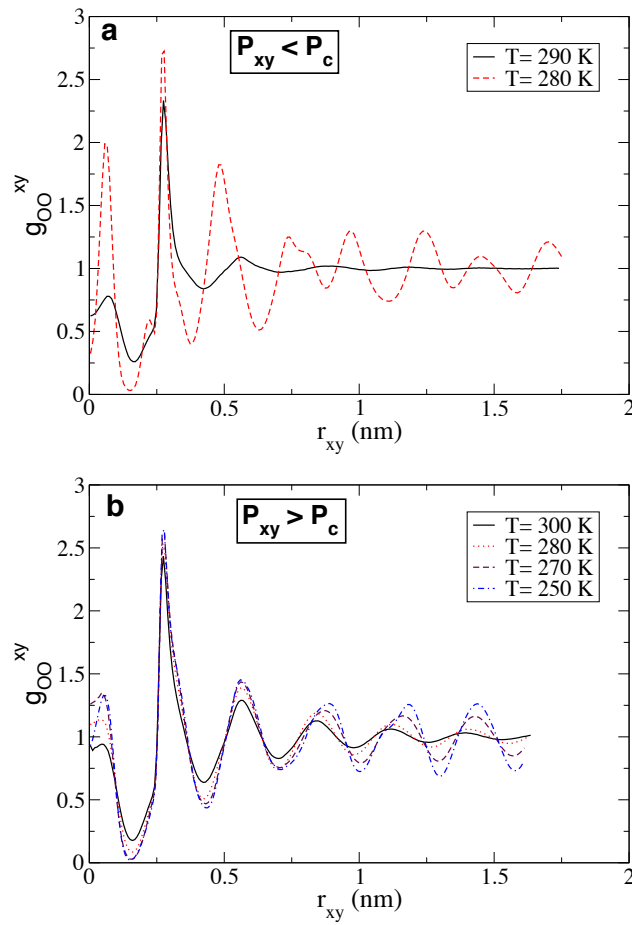


FIG. 7: Lateral oxygen–oxygen radial distribution function  $g_{OO}^{xy}$  as a function of lateral distance  $r_{xy}$  for **a.**  $P_{xy} < P_c$  and **b.**  $P_{xy} > P_c$ .